CHAPTER 7

DYNAMIC GAS DISENGAGEMENT

In this chapter, a new model for determining bubble sizes and specific interfacial areas in bubble columns by the dynamic gas disengagement (DGD) technique is developed, based on a concept of non-uniform steady state distribution of the bubble dispersion. Interpreting the non-uniformity in the axial direction, this model using the DGD technique gives axial gas holdup distributions, and by assuming an axially homogeneous dispersion, a radial gas holdup distribution can be obtained.

The Sauter mean diameters and specific interfacial areas for several gas-liquid systems have been estimated by the model and the DGD technique. The results in the air-water system are compared and are in agreement with those measured by a five-point conductivity probe technique. The obtained axial gas holdup distributions agree well with those measured by Menzel (1989) and the radial gas holdup distributions for the same system are also in reasonable agreement with those measured in this work. Results are also reported for the air-salt water, air-aqueous propanol and air-dodecylbenzene systems.

7.1 Introduction

A good understanding of the gas holdup structure, bubble rise velocities and bubble size distribution in bubble column reactors is essential for evaluating the

performance of such reactors. For determining the bubble size distribution, many methods have been developed. The photographic technique has often been used because of its simplicity (*e.g.* Towell *et al.*, 1965; Akita and Yoshida, 1974). This is a direct technique, but usually limited to bubbles in the vicinity of the column wall making it only suitable for low superficial gas velocities with little or no circulation. Obviously, it is also limited to transparent vessels. Other methods involve various electrical and optical probe techniques (Burgess and Calderbank, 1975; Buchholz *et al.*, 1981; Yu and Kim, 1990). These methods can measure not only bubble sizes, but also bubble velocities and local void fraction. However, in many cases, *e.g.* non-transparent, pilot-scale and industrial-scale columns, operating conditions of high temperature or high pressure as well as adverse system properties like low conductivity and high turbidity, may make it impossible to use these methods. In addition, for the purpose of obtaining global information for a whole column, these methods may be costly, laborious and time-consuming.

A convenient method to investigate the hydrodynamics of bubble column reactors, referred to as the dynamic gas disengagement technique (DGD), has been introduced by Sriram and Mann (1977). The basic idea of the technique is to obtain the rise velocities and the gas holdup structure of the bubble classes through analyzing the transient dispersion level profiles, recorded after gas flow is interrupted. If a relationship between the bubble rise velocity and the bubble size is known, it is possible to estimate the bubble size distribution from the velocity data. When only global information, *e.g.* the overall specific interfacial area, is to be obtained, this technique may be useful and effective.

Sriram and Mann (1977) used the technique in an air-water system at low superficial gas velocity (0.02 m/s) and low gas holdup (<5%), based on the two assumptions that there was no bubble-bubble interaction (e.g. coalescence of bubbles) once the gas supply was cut off, and that the dispersion was axially homogeneous prior to gas flow interruption. However, the method for predicting bubble size distributions was quite ambiguous, since the disengagement data were fitted to various bubble size distributions by tuning the mean and the standard deviation with or without consideration of liquid circulation and gas slugging. For example, without considering liquid circulation, a log-normal dis-

tribution of bubble sizes with a mean of 26.2 mm and a standard deviation of 8 mm was obtained by best fitting for a set of disengagement data. Considering liquid circulation, but without considering slugging, a log-normal distribution with a mean of 5 mm and a deviation of 1 mm could be obtained for the same disengagement data, when all bubble sizes in the column were assumed to be in range of 3-8 mm. A normal distribution was found to be incapable of fitting the disengagement data.

Based on the main assumptions proposed by Sriram and Mann (1977), further work has been done by other investigators, but not all of them have correlated the disengagement data to bubble size distributions. Vermeer and Krishna (1981) used the dynamic gas disengagement technique on the nitrogen-turpentine 5 system at high superficial gas velocities (up to about 0.3 m/s). They proposed a bimodal distribution with a successive disengagement process of a large bubble class as the transport portion and a small one as the entrained part. For the system used, this model showed the large bubbles to have a high gas volume fraction (e.g. about 1/3 of the total gas holdup) and a very high rise velocity (up to 1.8 m/s) in the heterogeneous flow regime.

Sasaki *et al.* (1986) proposed a multi-modal distribution of bubble sizes together with an assumption of a successive disengagement process, similar to that of Vermeer and Krishna (1981). In order to determine the bubble size, they simply assumed that the rise velocity of a bubble was proportional to its size. The method was used for determining bubble sizes in the system of argon and aqueous solutions of sodium hexadecyl sulfate in a small column (800 mm tall and 26 mm inner diameter), and the results were compared with data based on the photographic technique.

Schumpe and Grund (1986) have given a detailed discussion about how to obtain more accurate disengagement profiles, notably for the initial period of disengagement and also how to consider effects of the pressure difference across the distributor. The authors proposed a simultaneous disengagement and bimodal distribution model, and assumed that a bubble class had a constant slip velocity in both the steady state and during the dynamic disengagement process. This model implied that the first disengagement line was made up by contributions

from two bubble classes.

Patel *et al.* (1989) considered both successive and simultaneous disengagement models for bimodal distributions and expanded these to multi-modal distributions. In their models, a bubble class was assumed to have a constant rise velocity and a constant void fraction during its disengagement process. The authors preferred the simultaneous disengagement, although they expected the real process to lie between the two extremes. The bubble sizes were estimated from the obtained rise velocity data by assuming that a bubble class would rise as if this were the only bubble class existing in the liquid. The simultaneous model has been used to determine bubble sizes in the nitrogen-molten wax system (Patel *et al.*, 1990; Delay *et al.*, 1992). However, the sizes of the large bubble classes estimated by the simultaneous model for the air-water system at higher gas superficial velocities seem too large (sometimes they might be found to exceed the column diameter), and the results by the successive model were even worse. The results are also in contradiction with those measured by probe techniques (Yu and Kim, 1990), showing very low gas volume fractions for bubbles with such high rise velocities.

Lee *et al.* (1991) proposed a simultaneous disengagement model for multi-modal distributions using the assumptions of constant velocity and gas holdup. They derived the same expression of rise velocities for the various bubble classes as that of Sasaki *et al.* (1986) by using a gas volume balance during the disengagement process. The model was used for fermentation media systems in the determination of bubble velocities, but not for bubble sizes.

Unfortunately, none of the above models for the DGD technique can give a good estimation of the bubble size distribution or specific interfacial area in bubble columns. The main reason may be that the basic assumption (axially and radially homogeneous dispersion) used for the models is far from the true conditions, especially at higher superficial gas velocities.

This chapter is aimed at developing a new model in which the non-uniformity of the dispersion is considered when determining gas holdup structure and bubble rise velocities by the DGD technique.

7.2 Experimental Technique and Data Treatment

The dynamic gas disengagement measurements were carried out in a plexiglass column with inner diameter 0.288 m and height 4.33 m, equipped with the distributor having 250 holes (1 mm i.d.) for gas and 19 holes (28 mm i.d.) for liquid. The systems used were air-tap water (about 10-50 °C), air-dodecylbenzene, air-salt water and air-aqueous propanol solutions. A video-camera equipped with a timer and a VCR unit was used to record the drop in dispersion level during the disengagement process. After achieving steady state at a given gas superficial velocity, the gas flow to the column was cut and the drop in liquid level was recorded. The disengagement data were produced from frame-by-frame scanning of the video tape. The scanning procedure was repeated several times in order to minimize errors. However, the video-camera measuring technique was not successful at higher superficial gas velocities for the air-salt water and air-aqueous propanol solutions as these systems are nearly non-coalescing and easily foaming.

During the initial period of disengagement, at high superficial gas velocity, the liquid surface tended to fluctuate strongly and was often not clearly defined. The common practice of fitting a straight line is thus error prone unless multiple scanning of the tape is made; a procedure that is very time-consuming. Several alternatives have been suggested in the literature for measuring the disengagement profiles. Lee *et al.* (1985) introduced a digital dynamic gas disengagement sensor with a wooden buoy which could suppress some of the surface fluctuations. Weimer *et al.* (1985) used a γ-radiation density gauge to obtain the height of a fluidized bed as a function of time after cutting off gas supply. Sasaki *et al.* (1986) used a pressure transducer placed at a fixed position below the meniscus. Recently Daly *et al.* (1992) also used a pressure transducer for surface level measurements in stainless steel columns. These above methods not only improve measurement accuracy and reduce the work load, but can also be used in cases such as with non-transparent columns or liquid media, and in highly foaming systems.

A disengagement profile usually looks as shown in Figure 7.1a, which is a curve

showing the dispersion level as a function of the time after gas flow interruption. This can usually be fitted by a sequence of straight lines with decreasing negative slopes. The number of straight lines needed for the fitting depends on the gas-liquid system and the flow regime. For low and nearly non-coalescing systems such as air-aqueous propanol solutions and air-salt water, at low superficial gas velocities (with low gas holdup), referred to as the homogeneous flow regime, one straight line may be satisfactory. In the transition or heterogeneous regimes, more than one line were usually required. For systems like air-dodecylbenzene, at least three or more straight lines were necessary.

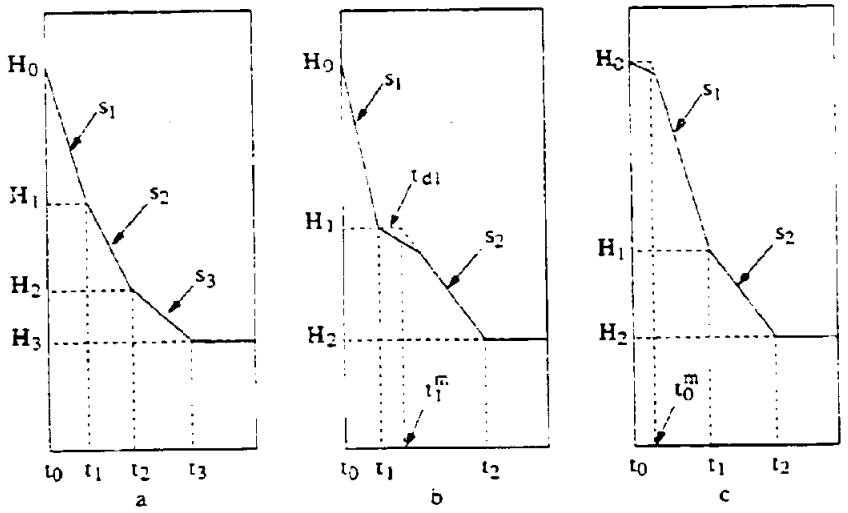

Figure 7.1 Sketch of the DGD profiles.

In our measured disengagement profiles, usually in the transition or heterogeneous flow regimes, it was found that there might exist a "buffer period" between two disengagement periods. In the buffer period, the drop rate of the liquid surface is slower than that of the subsequent period, as shown in Figure 7.1b. In fact, similar phenomena could also be observed when studying previous work (especially in high viscosity systems *e.g.* CMC solutions used by Schumpe and Deckwer, 1982), but they were usually ignored by the authors.

This phenomenon shows that liquid layers with fewer bubbles or lower void fraction may form during a disengagement process, as shown Figure 7.2c. This layer may be the result of rapid disengagement of larger bubbles and will contain a bubble size distribution representative of the next bubble class, although at a lower gas fraction. Thus, this part of the holdup may simply be added into the next disengagement period. For example, it can be considered that the second disengagement period starts at height H_1 and at time t_1^m, as shown in Figure 7.1b. The time difference, $t_{d,1} = t_1^m - t_1$, is the time delay after disengagement period 1.

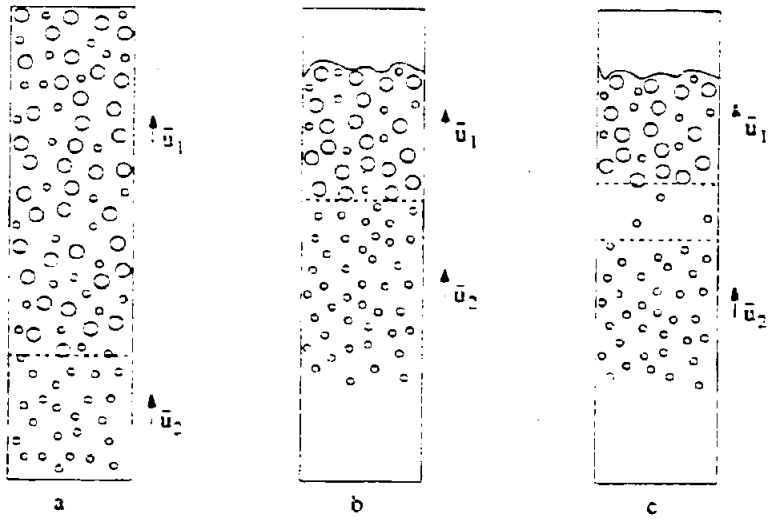

Figure 7.2 Sketch of bubble disengagement process.

At high gas throughput, a short buffer period may also appear at the beginning of the disengagement process, as shown in Figure 7.1c. Schumpe and Grund (1986) attributed this to the effect of the pressure drop through the gas distributor openings. Obviously, this effect will be significant only when the volume of the distributor chamber is large and the orifice gas velocity is high. However, even for a small distributor chamber at the moment of cutting off gas supply, the system is switched into dynamic operation and the rising bubbles will suddenly experience an additional downward liquid flow compared to at steady state.

Therefore, the apparent disengagement may be slow at the beginning, somewhat like a time delay, but will soon reach its mean value due to rapidly increasing gas void fraction near the surface (the effect can not easily be observed at low superficial gas velocities). The effect of the downward liquid flow is more significant for the bubbles at the top, because the surface bubbles burst with a lower rate than the rise rate of the bubbles (Azbel, 1981). As for the other buffer periods, this part of the holdup may be added to the first disengagement period. This implies that the disengagement is considered to start at time t_0^m instead of t_0. However, since the liquid surface often fluctuates strongly and therefore may not be clearly defined at the beginning of a disengagement process, this time delay can usually be disregarded, as done by the previous authors mentioned above.

Information for the air-tap water system measured by the five-point conductivity probe technique (Burgess and Calderbank, 1975; Buchholz *et al.*, 1981) will be used as comparison to the results by the DGD technique. This technique has relatively high accuracies for determining the equivalent bubble size and the rise velocity.

7.3 Holdup Structure and Rise Velocities

A bubble column reactor typically contains a large number of bubbles. Generally, when an experimental disengagement profile can be fitted by n straight lines, n disengagement periods and n bubble classes can be considered to exist. The bubble classes are numbered in decreasing order of bubble size. That is, the first bubble class represents the largest bubbles and the nth bubble class the smallest bubbles. Since a larger bubble class has a higher rise velocity, it will disengage from the liquid before the smaller bubble classes. In other words, in period j, only bubbles from the nth to the jth classes remain in the liquid, while bubbles from the j-1th to the 1st classes have escaped from the liquid before the start of the period.

In the dynamic gas disengagement technique, the first part consists of using the data for obtaining bubble rise velocities and the gas holdup structure of the various bubble classes, reflecting the characteristics of the corresponding steady state. In order to do this, as already mentioned, two basic assumptions have usually been used: (i) The gas holdup structure remains undisturbed by or without bubble interactions after cutting off the gas supply, and (ii) the holdup is axially uniformly distributed in the whole column prior to gas interruption (Sriram and Mann, 1977; Schumpe and Grund, 1986; Patel *et al.*, 1989).

Although the first assumption is considered to be necessary in order to make the data from the DGD technique representative of those of the corresponding steady state, it is difficult to accept the concept "without bubble interactions after interruption of gas supply". However, that "the gas holdup structure remains undisturbed by bubble interactions" may be acceptable for most systems, if it can imply that the bubble coalescence and breakup process still remain in balance during the disengagement process and that they are, during the first period, close to the situation in the steady state.

The second assumption is more critical except for non- or low coalescing systems at low superficial gas velocities (the homogeneous flow regime or highly turbulent bubbling regime). Indeed, for instance, for the air-salt water system, when the superficial gas velocity was high, it was observed that large aggregates of bubbles occurred, rising fast in the upper part of the column and making the overall gas holdup decrease. At slightly lower superficial velocities, the gas holdup was found to be very high and the system became foaming. For a system with coalescence promoting liquids, the axial variation of bubble sizes is usually strong in the vicinity of the distributor. The gas holdup may be lower at the sparger if the gas is not uniformly distributed and it is generally higher in the disengagement zone at the top (Schumpe and Grund, 1986). In tall columns, the gas expansion due to the variation in hydrostatic head may also have to be considered. The experimental results of Ueyama *et al.* (1980) have shown that there exists a clear axial inhomogeneity in the gas holdup for the air-water system in a column with inner diameter 0.6 m and height 3 m. This has also been experimentally verified by Menzel (1989) for both low and high coalescing systems in a column with inner diameter 0.6 m and height 5 m.

On this background, the present model assumes that prior to gas interruption, only the smallest bubble class is axially uniformly distributed over the whole height of the column, and that each of the other bubble classes has an axially uniform distribution only over a limited height from the top, as shown in Figure 7.2a. It should also be kept in mind that the gas holdup in reality is non-uniformly distributed in the radial direction.

The present model assumes that the gas holdup for a bubble class is constant during a disengagement process or, in other words, that the bubble classes disengage independently of each other with constant rise velocities, as also done by other investigators (*e.g.* Patel *et al.*, 1989; Lee *et al.*, 1991). Clearly, this is an oversimplification. In a disengagement process, as the bubbles leave the lower part of the column, their volume has to be replaced by liquid. The resulting downward flow of liquid will affect the bubble rise velocities, especially those of the smaller bubbles. However, smaller bubbles will be carried along in the wakes of larger bubbles counteracting the reverse liquid flow effect. Hence, the approximation that the bubble classes disengage independently of each other with constant velocities, may appear reasonable considering that the desired information is only for a few distinct bubble classes, which in itself is a substantial simplification.

Thus, the total volume of bubbles disengaged in period j, $-s_j\Delta t_j A_c$, is composed of all the bubble classes disengaging in this period. Corresponding to the disengagement rate of bubbles from the liquid surface, the surface level drops with velocity s_j from height H_{j-1} to H_j within the same time interval, $\Delta t_j = t_j - t_{j-1}$. Considering each of the bubble classes having a constant rise velocity in the disengagement process, and that no bubble class larger than the jth exists in period j, and ignoring the density difference between gas over and below the surface, a mass balance for gas in the period gives

$$\sum_{i=j}^{n} (u_i - s_j)\varepsilon_{Gi} = -s_j, \quad j = 1, \ldots, n \tag{7.1}$$

Here u_i is the rise velocity of bubble class i and ε_{Gi} is its holdup, both being

constant in the whole disengagement process.

Equation (7.1) can be rewritten as

$$\sum_{i=j}^{n} u_i \varepsilon_{Gi} = -s_j(1-\bar{\varepsilon}_{Gj}) \tag{7.2}$$

where

$$\bar{\varepsilon}_{Gj} = \sum_{i=j}^{n} \varepsilon_{Gi} = \varepsilon_{Gj} + \bar{\varepsilon}_{Gj+1} \tag{7.3}$$

is the total gas void fraction in the top disengagement zone in period j.

A relative superficial gas velocity for each of the bubble classes (superficial velocity relative to the liquid surface instead of the wall), $(u_i - s_i)\varepsilon_{Gi}$, can be obtained from Equations (7.2) and (7.3) as follows

$$(u_i - s_i)\varepsilon_{Gi} = (-s_i + s_{i-1})(1-\bar{\varepsilon}_{Gi-1}) , \quad i = 1,\ldots,n \tag{7.4}$$

where $s_{n+1} = 0$ and $\bar{\varepsilon}_{Gn+1} = 0$. Since the rise velocity, u_i, and the gas holdup, ε_{Gi}, are constant for a bubble class in the disengagement process, the relative superficial velocity is also a constant.

On the other hand, the disengaging dispersion can be considered to consist of several distinct moving layers containing different numbers of bubble classes at any time. For instance, there are two distinct layers in the case of Figure 7.2. The first layer contains two bubble classes. Each of the layers rises with an apparent velocity equaling the average rise velocity in the corresponding period, since both the rise velocities and the holdup are constant. Thus the apparent velocity can be expressed by

$$\bar{u}_i = -s_i \frac{1-\bar{\varepsilon}_{Gi}}{\bar{\varepsilon}_{Gi}} \tag{7.5}$$

If the velocities of any two adjacent layers (or periods) are equal, the disengagement dispersion is continuous, as shown in Figure 7.2b. Otherwise, a layer of nearly bubble-free mixture will be formed, as shown in Figure 7.2c (see the discussion in the above section). The velocities will have the following relationship

$$(\bar{u}_i - \bar{u}_{i-1})t_i = \bar{u}_{i-1}t_{d,i} \tag{7.6}$$

where $t_0 = 0$ has been used and $t_{d,i}$ is the time delay after disengagement period i, which can be determined as shown in Figure 7.1b. Both sides of the above equation represent the thickness of the bubble-free layer.

Combining Equations (7.5), (7.3) and (7.6), the void fraction for bubble class i is

$$\varepsilon_{Gi} = \frac{-s_i}{-s_i + \bar{u}_{i-1}(1 + t_{d,i}/t_i)} - \bar{\varepsilon}_{Gi-1} \tag{7.7}$$

Then the rise velocity for the bubble class, u_i, can be determined by the above equation and Equation (7.4):

$$u_i = \frac{(-s_i + s_{i-1})(1 - \bar{\varepsilon}_{Gi-1})[-s_i + \bar{u}_{i-1}(1 + t_{d,i}/t_i)]}{-s_i(1 - \bar{\varepsilon}_{Gi-1}) - \bar{u}_{i-1}\bar{\varepsilon}_{Gi-1}(1 + t_{d,i}/t_i)} + s_i \tag{7.8}$$

Equations (7.7) and (7.8) indicate that the void fraction and rise velocity for bubble class i can be calculated from the total void fraction and the apparent velocity in the next disengagement period, $\bar{\varepsilon}_{Gi-1}$ and $\bar{u}_{i-1}$, if they are known.

For the smallest bubble class, it rises from the bottom and has travelled a distance H_n at the end of a disengagement process. Hence, its rise velocity can be determined by

$$u_n = \bar{u}_n = H_n/t_n \tag{7.9}$$

Then, the void fraction of the smallest bubble class can directly be calculated from Equation (7.5):

$$\varepsilon_{Gn} = \bar{\varepsilon}_{Gn} = \frac{-s_n t_n}{-s_n t_n - H_n} \tag{7.10}$$

In Equations (7.9) and (7.10), it has been assumed that the last layer contains only the smallest bubble class. Hence the rise velocity and void fraction for this bubble class are equal to the apparent rise velocity and total void fraction in the last disengagement period.

7.4 Non-Uniform Distribution

A coefficient for the non-uniformity of gas holdup is introduced to describe the originally axial distribution of a bubble class in the column. The coefficient, ξ_i, is defined such that a bubble class i is distributed in the distance, $H_0\xi_i$, from the top prior to the gas interruption. Knowing the rise velocities and void fractions for all bubble classes, these coefficients can be calculated. The assumption that the smallest bubble class is distributed over the whole height of the column directly gives $\xi_n \equiv 1$.

According to Equation (7.4), the disengaged volume for bubble class i can be calculated by

$$v_{Gi} = A_c(-s_i + s_{i-1})(1 - \bar{\varepsilon}_{Gi-1})\sum_{j=1}^{i} \Delta t_j \tag{7.11}$$

where $\Delta t_j = t_j - t_{j-1}$. For a disengagement profile without any "buffer period" or delay time, as described in the experimental section, the term in the above equation, $\sum \Delta t_j$, will equal t_i. Hence, the disengaged volume can be simplified to be

$$v_{Gi} = A_c(-s_i + s_{i-1})(1 - \bar{\varepsilon}_{Gi-1})t_i \tag{7.12}$$

Then the void fraction for a bubble class can be expressed as

$$\varepsilon_{Gi} = \frac{v_{Gi}}{A_c H_0 \xi_i} \tag{7.13}$$

This equation is also used to determine the non-uniform distribution coefficient, ξ_i, when ε_{Gi} is known.

7.5 Bubble Size and Specific Interfacial Area

Having obtained rise velocities for the n bubble classes from the above analysis, it may be possible to estimate the corresponding bubble size for each of them if a relationship between the rise velocity and the terminal velocity can be found. Patel *et al.* (1989) used the rise velocities of the bubble classes obtained by their DGD model as those of a bubble swarm in quiescent liquid at steady state, and then corrected them to the corresponding terminal velocities of single bubbles based on a relationship proposed by Marrucci (1965). This estimation method is simple, but may be questionable, since the velocities are directly obtained from the dynamic state where the effect of the downward flow of liquid is added compared to the corresponding steady state.

It may be more reasonable to think that the relative velocity between bubble and liquid for a given bubble size is the same in both the dynamic and the steady state. The relative velocity of a bubble class can be calculated from its rise velocity, u_i, as given by the analysis presented above, and the downward liquid flow rate. However, the real downward liquid flow rate around the bubble class is unknown. A way to solve the problem is to substitute the average downward liquid flow rate, which is known but varies with disengagement period (*e.g.*, the average downward velocity of liquid is $-s_i$ in period i), for the real one.

As already stated, the present model assumes a constant rise velocity for the whole disengagement process. Hence, in order to be consistent, the relative velocity of a single bubble class must be taken as the average relative velocity over all periods, when the average downward liquid flow rate is used. A simple consideration is to take the time averaged velocity of a bubble class relative to the average downward velocity of liquid in the whole disengagement process as the characteristic relative velocity of the bubble class. This gives

$$u_{ri} = \frac{\sum_{j=1}^{i}(u_i - s_j)\Delta t_j}{\sum_{j=1}^{i}\Delta t_j} = u_i + (H_0 - H_i)/t_i \tag{7.14}$$

When the relative velocity, u_r, is considered as the terminal velocity, the corresponding equivalent diameter may be calculated by known correlations about terminal velocities of single bubbles. The terminal velocity correlation proposed by Fan and Tsuchiya (1990) is used in this work, since it covers a broad bubble size range. The correlation is

$$\tilde{u}_t = \left[\left(\frac{Mo^{1/4}k_b}{\tilde{d}_e^2}\right)^{k_n} + \left(\frac{2k_c}{\tilde{d}_e} + \frac{\tilde{d}_e}{2}\right)^{-k_n/2}\right]^{-1/k_n} \tag{7.15}$$

where

$$\tilde{u}_t = u_t\left(\frac{\rho_L}{g\sigma}\right)^{1/2}, \quad \tilde{d}_e = d_e\left(\frac{\rho_L g}{\sigma}\right)^{1/2} \tag{7.16}$$

The parameters k_b, k_c and k_n are system dependent. For instance, Fan and Tsuchiya (1990) recommend $k_b = 37.2$, $k_c = 1.2$ and $k_n = 0.8$ for the air-tap water system.

Knowing the bubble sizes and holdups for various bubble classes, the Sauter mean diameter and the specific gas-liquid interfacial area can be calculated by

$$d_s = \frac{\sum_{i=1}^{n} v_{Gi}}{\sum_{i=1}^{n} v_{Gi}/d_{ei}}, \quad a = 6\sum_{i=1}^{n} \frac{v_{Gi}}{H_0 A_c d_{ei}} \tag{7.17}$$

7.6 Results and Discussion

7.6.1 Bubble size and interfacial area

As an example, the relative velocities, holdup structure and equivalent bubble sizes calculated from the DGD data of the air-tap water system, according to this model, are shown in Table 7.1. It is found that at low superficial gas velocities, two bubble classes are usually obtained. At high superficial gas velocities, a division into more than two bubble classes is required (the air-salt water system is similar). The higher the superficial velocities, the larger the gas holdup and the sizes of the large bubble classes. However, the holdup for bubbles larger than 10 mm is always small, and most of the bubbles are in the size range 4-6 mm. This agrees with the results measured by the probe technique (Yu and Kim, 1990; Yao *et al.*, 1991).

The Sauter mean diameters and the specific interfacial areas at various superficial gas velocities for the air-tap water system are calculated from the DGD model and are shown in Figure 7.3 and Figure 7.4. The results are compared with our measured results from the five-point probe technique and calculated results according to the correlations of Akita and Yoshida (1974). These correlations are based on the photographic technique and therefore known to be suitable only in the homogeneous regime (Deckwer, 1992). This is also verified by the figures.

Table 7.1 Relative velocities, bubble sizes and holdup structure for the air-tap water system by the DGD technique.

u_G (cm/s)	u_r (cm/s)			d_{ei} (mm)			$\varepsilon_G/(A_cH_D)$ (%)		
2.23			22.5			5.91			13.3
2.51			22.4			5.63			14.1
4.51		22.2	22.1		5.18	4.73		2.66	16.8
5.64		22.6	22.2		6.12	5.09		4.81	19.2
6.70	22.9	22.5	22.0	6.65	5.92	4.32	2.38	3.41	19.9
7.93	25.8	22.6	22.3	11.2	6.19	5.29	1.24	3.54	18.1
9.31	27.1	22.2	22.0	13.0	5.10	4.42	1.20	2.28	17.5
12.3	29.6	28.6	22.2	13.1	11.6	5.01	2.33	1.57	17.4
14.3	31.6	28.1	22.1	19.2	14.3	5.15	2.61	4.49	16.2
17.0	33.7	32.8	22.4	22.1	20.8	5.80	2.16	6.08	16.5

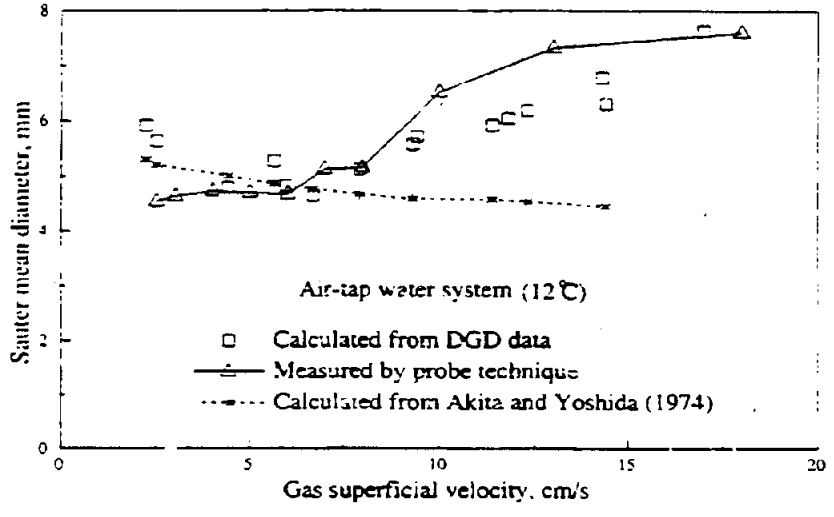

Figure 7.3 Sauter mean diameters obtained by the DGD technique and measured by the probe technique for the air-tap water system.

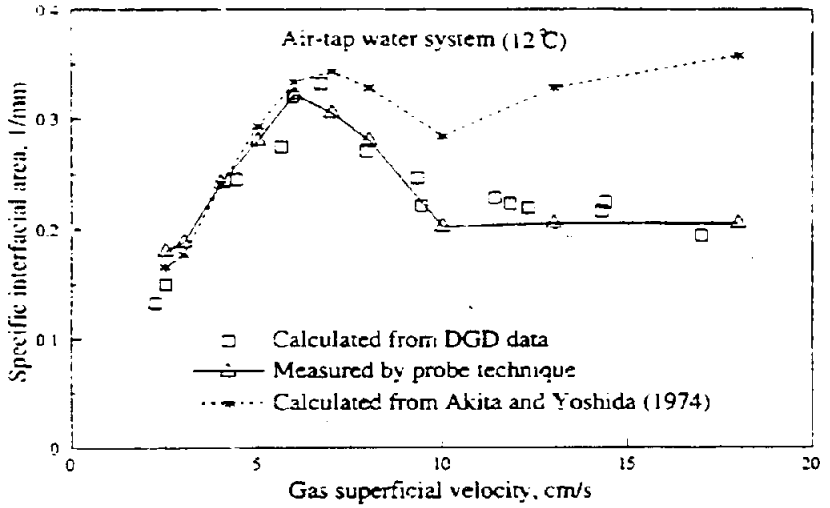

Figure 7.4 Specific interfacial area obtained by the DGD technique and measured by the probe technique for the air-tap water system.

At low superficial gas velocities, both the Sauter mean diameters and the specific interfacial areas obtained from the three methods are close. However, at high superficial gas velocities, the results estimated by the present DGD model and measured by the probe technique are in fair agreement, while the Sauter mean diameters obtained from the correlation of Akita and Yoshida (1974) are too small, and thereby the specific interfacial areas too large.

The specific interfacial area is found to increase with the superficial velocity up to a maximum and then to decrease. At superficial velocities above 10 cm/s, the interfacial area becomes almost constant. The reason for this is the fast increase in the overall gas holdup with superficial gas velocity in the homogeneous flow regime (here u_G < 5-6 cm/s), while the Sauter mean diameter remains nearly constant or increases only slowly in this regime. As the superficial gas velocity increases further, the overall holdup stabilizes and goes down whereas the Sauter mean diameter increases fast due to the effect of coalescence in the transition regime ($5 < u_G < 10$ cm/s), leading to a fast reduction in the specific interfacial area. In the heterogeneous regime it again stabilizes due to the renewed increase

in overall gas holdup and the continued increase of the Sauter mean diameter.

Figure 7.5 gives the bubble rise velocity and the cumulative volume percentage measured by the five-point conductivity probe technique at two levels of superficial gas velocity in the air-water system. Comparing the figure to Table 7.1, it is found that the bubble rise velocities measured by the probe are higher than those estimated by the DGD technique. This is not surprising since the velocities measured by the probe include the effect of liquid or wake velocities, while the estimated ones by the DGD model are the relative velocities between the bubbles and the liquid.

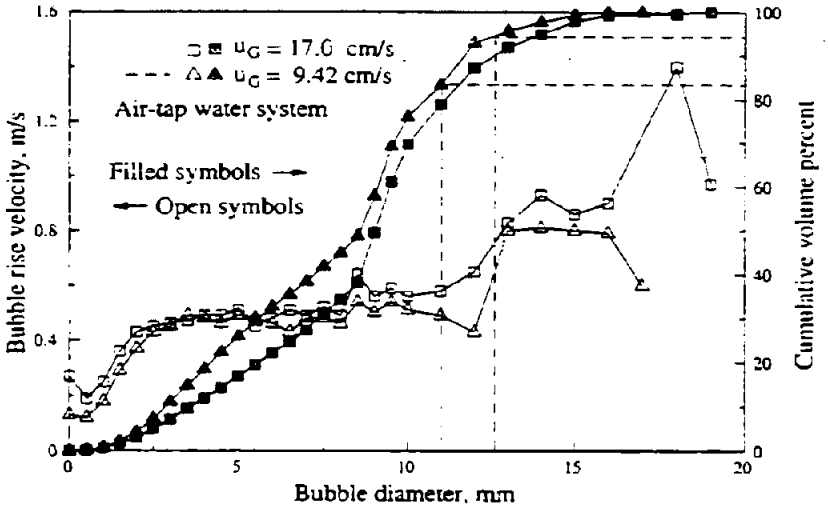

Figure 7.5 Bubble volume fraction and rise velocity measured by the probe technique and compared to the results by the DGD technique.

The classification of bubble sizes for the DGD technique is founded on bubble sizes grouping by similarity in bubble rise velocity. Figure 7.5 shows that the results measured by the five-point conductivity probe technique for the air-water system support this classification. For example for u_G = 17 cm/s, the volume fraction of the smallest bubble class (d_s = 5.8 mm) is about 67%, calculated from

Table 7.1. According to the results of the probe technique, this percentage identifies the bubble class consisting of the bubbles smaller than 9.8 mm with a nearly constant rise velocity of about 50-57 cm/s. The volume fraction of the largest bubble class is 8.7% and this bubble class comprises bubbles larger than 12.8 mm with a nearly constant rise velocity of about 90 cm/s. The second bubble class (volume fraction 24.5%) is in the size range 9.8-12.8 mm with rise velocities varying between 52-89 cm/s. For u_G = 9.4 cm/s, the smallest bubble class has 83.4% of the total gas volume and correspondingly covers bubble sizes up to 11 mm with a nearly constant rise velocity of 48-52 cm/s. The largest one has 5.7% of the total gas volume and contains bubbles larger than 12.6 mm with a constant rise velocity 80 cm/s. The second bubble class covers bubble sizes of 11-12.6 mm. In fact for this gas flow rate, the second bubble class from both Figure 7.5 and Table 7.1 can be incorporated into the first one, according to the velocity classification. For both of the gas velocities, the classifications in bubble size according to Figure 7.5 and Table 7.1, are seen to compare well, in particular for the lower gas flow rate.

For the air-dodecylbenzene system, the disengagement profiles are closer to continuous curves and thereby more fitted straight lines are necessary (usually 4-6 lines). The calculated Sauter mean diameters and the specific interfacial areas for various superficial gas velocities are shown in Figure 7.6. The Sauter mean diameter increases with the superficial gas velocity throughout the whole range tested. The specific interfacial area increases with the gas velocity at low velocities, but levels off and decreases at high superficial gas velocities. The reason is similar to that for the air-tap water system. Both the Sauter mean diameter and the overall gas holdup increase with the superficial velocity. The increase in the Sauter mean diameter is slow at low superficial velocity. However, unlike in the air-tap water system, this system has no transition regime, that is, the overall gas holdup does not decrease with the gas velocity. At high superficial gas velocity, the increase in the overall gas holdup becomes slower, whereas the Sauter mean diameter increases faster. This makes the interfacial area decrease.

The Sauter mean diameter and the specific interfacial area for the air-salt water solution system are shown in Figure 7.7. This is a typical non- or low coalescing

system. When the superficial velocity is low, the overall gas holdup, as usual, increases with the superficial velocity. However, the Sauter mean diameter decreases with the superficial gas velocity in the homogeneous flow regime due to the increase in turbulent intensity and thereby in bubble breakup. Hence, the specific interfacial area increases fast. At superficial velocities above about 5 cm/s, the system became foaming and the visual DGD technique failed to give results. However, when the superficial velocity was increased to about 10 cm/s, the overall gas holdup decreased due to the formation of large bubble aggregates in the upper portion of the column. This made measurements possible again and the interfacial area was found to decrease.

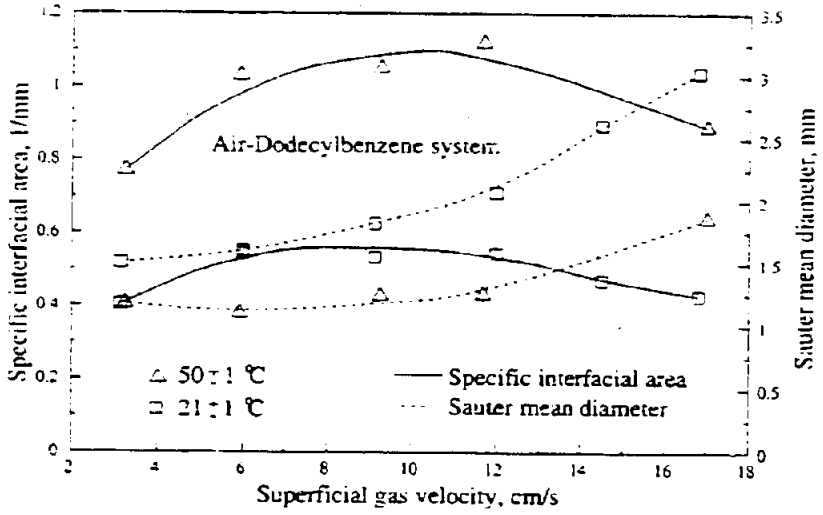

Figure 7.6 Specific interfacial area and Sauter mean diameter obtained by the DGD technique for the air-dodecylbenzene system.

Figure 7.8 shows the calculated Sauter mean diameters and the interfacial areas for the nitrogen-dimethylbenzene system from the data of Ullaland (1991). The data were analyzed according to a bimodal distribution (only two bubble classes exists in the system). The Sauter mean diameter initially decreases with the superficial gas velocity and then becomes stable. The interfacial area increases with the gas velocity.

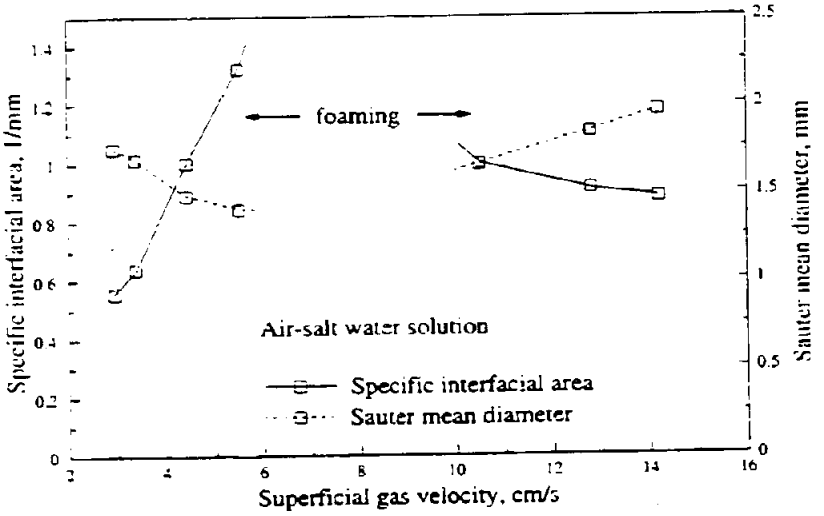

Figure 7.7 Specific interfacial area and Sauter mean diameter obtained by the DGD technique for the air-salt water solution system.

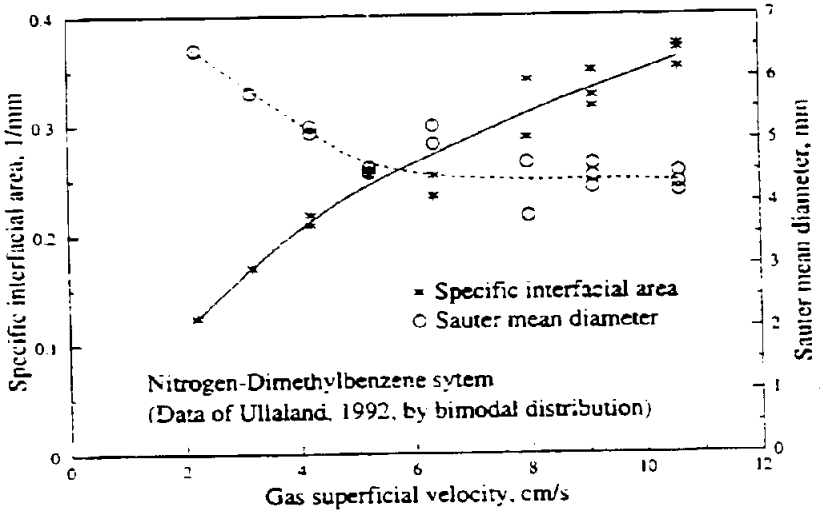

Figure 7.8 Specific interfacial area and Sauter mean diameter obtained by the DGD technique for the nitrogen-dimethylbenzene system.

It should be pointed out that all bubble sizes for the above systems are calculated based on the terminal velocity correlation of Fan and Tsuchiya (1990). In this correlation, the parameters, k_b, k_c and k_n, are system dependent and only those for the air-tap water system have been verified by them. For the other systems, the parameters used are calculated using the methods given by the same authors.

7.6.2 Non-uniform distribution

According to the concept of an axial non-uniform distribution coefficient, ξ_i, the holdup distribution can be calculated and is shown in Figure 7.9. It indicates that the higher the superficial gas velocity, the larger discrepancy from a uniform distribution in local gas holdup. The experimental results of Ueyama *et al.* (1980) also showed that high non-uniformity of the dispersion appeared at high superficial gas velocities.

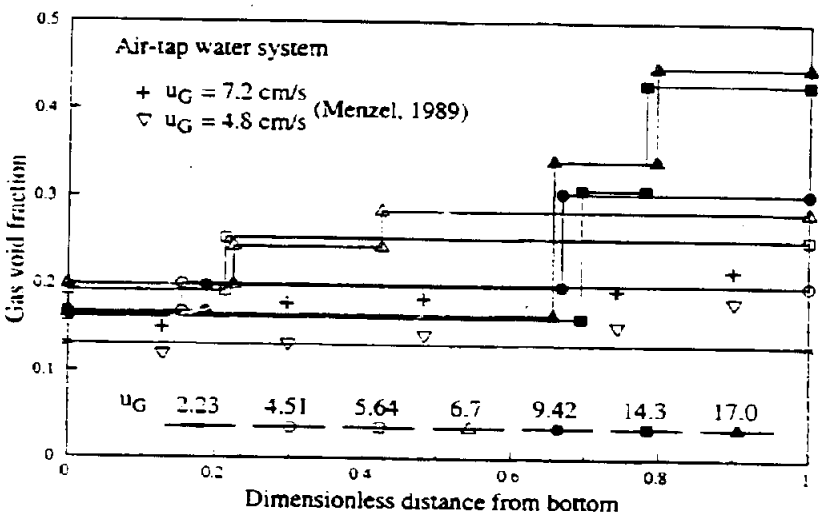

Figure 7.9 Axial distribution of gas holdup estimated by the DGD technique.

In order to compare the gas holdup distributions with those obtained by other techniques, the data measured by Menzel (1989) using the one-point conductivity probe technique for the same system in a column of 0.6 m inner diameter and 5.44 m height with the same type of distributor are directly plotted in Figure 7.9. Although the column diameter used by Menzel (1989) is different from that used in this work, the results may be comparable since the column diameter has a small effect on the gas holdup with column diameters larger than 0.1 m (Akita and Yoshida, 1974; Hills, 1974; Hikita *et al.*, 1980; Ueyama and Miyauchi, 1979). The trend of increasing gas holdup with the height is shown to be similar for the data from the DGD model and the measurements of Menzel (1989). Although discrepancies seem to exist according to Figure 7.9, Menzel (1989) has concluded that the gas holdup data measured by the one-point conductivity probe were underestimated by about 20%. If the corrected data of Menzel (1989) were shown in Figure 7.9, a good agreement would be found.

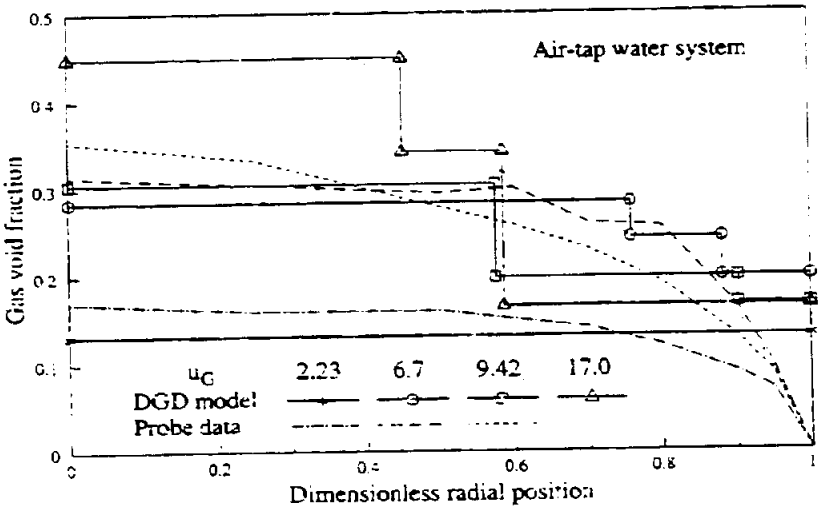

Figure 7.10 Radial distribution of gas void fraction estimated by the DGD technique.

Instead of interpreting the inhomogeneity in the axial direction, according to Equation (7.13), one may assume an axially uniform distribution over the whole height of the column, and then the coefficient, ξ_i, may be equivalent to indicate a non-uniform distribution in the radial direction. This means that bubble class i is distributed in area $\xi_i A_c$ from the central axis and thereby $\xi_i^{1/2} = r/R$ (dimensionless radial position in the cross-section). Figure 7.10 shows examples of the holdup distribution in the radial direction based on the above concept and comparisons with the results measured by the five-point conductivity probe technique. The calculated radial non-uniform distributions of gas holdup are seen to conform reasonably well with the measured results.

7.7 Conclusion

A new model to be used with the dynamic gas disengagement technique has been developed, based on the concept of non-uniform steady state gas holdup and bubble size distribution. The model is shown to predict the distribution of bubble classes, and thereby gas holdup, in agreement with experimental data. The distribution of gas holdups can be interpreted either as axial or as radial distributions, both of which agree reasonably with distributions determined by other experimental methods.

The present model shows that the classification of bubbles according to their rise velocities, which is the basis of the DGD technique, is reasonable and effective. This is also verified by the results measured by the five-point conductivity technique.

The bubble size distribution and the specific interfacial area have been deduced based on the assumption of a constant rise velocity for a given bubble class through the whole disengagement process. Integrating this as the swarm terminal velocity, Sauter mean diameters and specific interfacial areas could be determined in fair and good agreement respectively with those found experimentally, over a wide range of gas velocities (2-18 cm/s).

The Sauter mean diameter and interfacial area determinations are however sensitive to the accuracy of the relationship between bubble size and swarm terminal velocity and improved correlations for systems other than the air-water are needed.